Attitude Propagation Using Slewing and Rotational Transformations of a Single Axis

Russell P. Patera[1]

Abstract

The exact slewing attitude transformation of a single axis that moves along a conical trajectory was derived. The result was used to increase the attitude propagation accuracy using a single axis by incorporating the slewing motion of the angular rate vector into the attitude propagation algorithm. It was shown that when the slew rate of the angular rate vector has a fixed orientation in the body frame and has a magnitude proportional to the angular rate vector magnitude, the attitude can be propagated with only numerical roundoff error. The findings not only agree with previously published results, but provide and additional new solution due to the commutative property of the associated slewing and rotational transformations. The algorithm was applied to pure coning motion having time dependent angular rate magnitude and the coning motion of axisymmetric vehicles with time dependent angular rate magnitude. Numerical examples that demonstrate the improvement in accuracy are included.

Keywords: attitude propagation, coning error, axisymmetric vehicle, rotational transformation, slewing transformation, Pivot Vectors, quaternion

Nomenclature

A, B - slewing axis orientations

b - initial slewing axis orientation

c - final slewing axis orientation

I_T - transverse axis moment of inertia

I_S - spin axis moment of inertia

J - angular momentum vector

K - unit vector in direction of **α**, also the z-axis

q - vector part of quaternion

q(0) - scalar part of quaternion

R(**z**, λ) - rotational transformation about the z-axis

T - propagation time

U - general attitude transformation

$\mathbf{U_R}$ - rotational transformation

$\mathbf{U_S}$ - slewing transformation

$\mathbf{U_T}$ - total transformation

[1] Russell.p.patera@gmail.com

$\mathbf{V_1, V_2, V_3}$ - Pivot Vectors

X, Y, Z - coordinate axes

$\boldsymbol{\alpha}$ - angular rate vector of $\boldsymbol{\omega}$ in body frame

Δ - integral of ψ

ϵ - angle between slewing axis and $\boldsymbol{\alpha}$

λ - integral of angular rate magnitude

Ω - integral of α

ψ - magnitude of $\boldsymbol{\alpha}+\boldsymbol{\omega}$

Θ - angle between $\boldsymbol{\alpha}$ and $\boldsymbol{\omega}$, also polar angle

$\Delta\Theta$ - $\boldsymbol{\omega}\,\Delta t$

$\boldsymbol{\omega}$ - angular rate vector

$\boldsymbol{\omega_N}$ - component of $\boldsymbol{\omega}$ normal to $\mathbf{A}$

$\boldsymbol{\omega_T}$ - component of $\boldsymbol{\omega}$ parallel to $\mathbf{A}$

ϕ - polar angle, also integral of ω

Φ - Euler Rotation Vector

1. Introduction

A recent work found that the attitude of a vehicle can be propagated by considering a single axis that is fixed in the inertial frame but slews in the body frame, as it is driven by the body angular rate vector [Patera, 2020a]. During the slewing motion of the axis, the body rotates about the axis as it is driven by the component of the angular rate vector along the axis. The slewing and rotational transformations can be computed separately and their product yields the total transformation. It was also determined that the slewing transformation can be performed prior to or after the rotational transformation (Patera, 2020a), which provides two solutions to the propagation problem. The initial orientation of the axis alters the slewing transformation and the rotational transformation but not the total transformation. The resulting attitude propagation accuracy was found to be equivalent to accuracies obtained using other attitude representations, such as Euler angles, quaternions, etc. Since nearly all attitude propagation algorithms assume that the angular rate vector maintains a fixed orientation during each propagation time step, they suffer propagation error or coning error. Attitude propagation error is introduced by not accounting for the changing orientation of the angular rate vector during each propagation step. The resulting error can be reduced but not eliminated by shortening the duration of each propagation time step or by using more advanced numerical integration algorithms (Andrle, and Crassidas, 2013; Sveier, Sjoberg, and Egeland, 2019.)

Earlier works directly addressed this attitude propagation error by computing the slew angular rate vector of the angular rate vector and incorporating it into the attitude propagation algorithm (Patera, 2010, and Patera, 2011). Time dependent angular rate vector orientation was also included in the Pivot Vector method (Patera, 2017). The improved attitude propagation algorithms eliminated coning error for pure coning motion and greatly improve propagation accuracy for the general case. It was also shown to be effective in improving propagation

accuracy for a sequence of angular increments produced by strapdown inertial navigation units on flight vehicles (Patera, 2010).

The goal of the current work is to improve attitude propagation accuracy using a single axis by including information on the changing direction of the angular rate vector in the propagation algorithm. This is achieved by dividing the total propagation time into time intervals that have associated incremental slewing and rotational transformations. The duration of each propagation interval is sufficiently short, such that, the slew rate vector of the angular rate vector is in a fixed direction. As a result, the angular rate vector slews along a conical trajectory centered on the slew angular rate vector. A new analytical method to compute the slewing transformation of an axis that moves along a conical trajectory centered on a fixed axis was developed and used to obtain the exact slewing transformation. As a result, the associated rotational transformation also is exact. The product of the incremental slewing and rotational transformations yields the incremental attitude transformation, which is exact and free of coning error. The commutative property of the incremental slewing and rotational transformations results in two equivalent incremental attitude transformations that are valid for both fixed and time dependent angular rate vector magnitudes. One solution agrees with results from earlier works that were obtained using different methods (Patera, 2010 and Patera, 2011) and the other solution is a new result. The total attitude propagation is the product of the sequential incremental transformations spanning the total propagation time.

Section 2 presents a method to obtain the slewing transformation of a single axis fixed in the body frame that slews about an axis having a fixed orientation in the inertial frame. This method, which illustrates how to obtain error free propagation of a slewing axis, was previously applied to Foucault Pendulum kinematics (Patera, 2020b) and was used to derive the pendulum's precession frequency. The same method is used in this work to obtain the slewing transformation of an inertially fixed axis that slews in the body frame, as it is driven by the angular rate vector. Section 3 presents the main algorithm for attitude propagation that involves both the slewing and rotational transformations of an axis fixed in the inertial frame but slews in the body frame due to a slewing angular rate vector. The method is valid for slew rate vectors of the angular rate vector that have fixed orientation and have magnitude proportional to the magnitude of the angular rate vector. Section 4 presents the attitude propagation for an axisymmetric vehicle, which illustrates the result of Section 3. The resulting attitude transformation was also represented by Pivot Vectors and the related quaternion (Patera, 2017). Section 5 applies the results of Section 3 to the case of pure coning motion and propagates the associated attitude with only numerical roundoff error. Section 6 presents numerical results for the slewing transformation of an axis that slews along a conical surface about an axis of fixed orientation. Results are compared to those of a standard attitude propagation method that has fixed orientation of the angular rate vector during each time step. Section 7 presents numerical results for propagating the attitude of an axisymmetric vehicle with time varying angular rate magnitude. Propagation results using the proposed method are compared to those of a standard method. Section 8 presents the conclusions.

2. Slewing transformation of a single axis about a fixed axis

The slewing transformation of a single axis can be obtained by considering the total transformation generated by an angular rate vector of fixed orientation over a time interval. The total transformation is the product of desired slewing transformation and a rotational transformation about the slewing axis. Let Θ be that angle between the slewing axis, **A**, and the angular rate vector, **ω(t)**. If **z** is a unit vector aligned with **ω(t)**, and T is the propagation time interval, then the total transformation is given by **R**(**z**, λ) in eq. (1).

$$\mathbf{U} = \mathbf{R}(\mathbf{z},\ \lambda), \qquad \text{where} \quad \lambda = \int_0^T \omega(t)\, dt \tag{1}$$

Although the total transformation in eq. (1) indicates a body frame rotation by angle λ about the **z**-axis, it also can be represented as the product of a slewing transformation and a rotational transformation. The slewing transformation, $\mathbf{U_S}$, slews the axis from orientation **A** to orientation **B**, as shown in Fig. 1 and expressed in eq. (2).

$$\mathbf{B} = \mathbf{U_S}\,\mathbf{A} \tag{2}$$

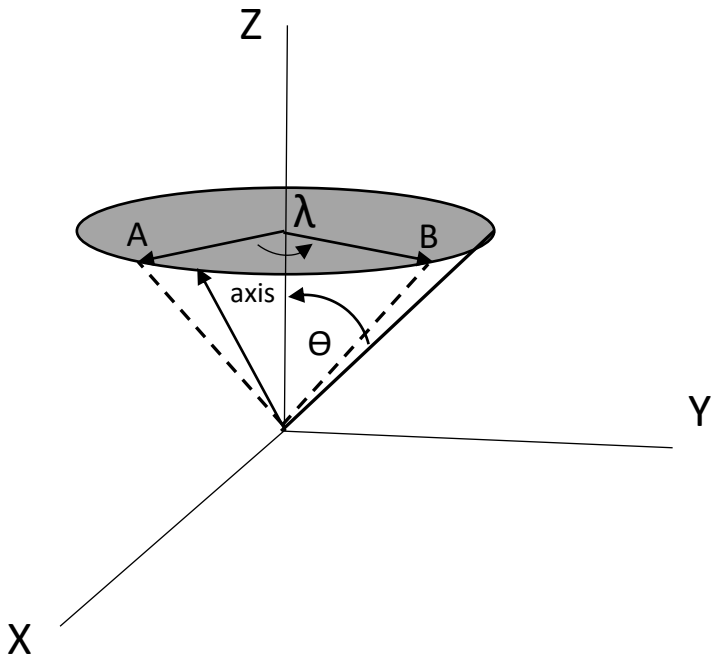

Fig. 1 Axis slewing from orientation **A** to orientation **B**.

The rotational transformation is a rotation of the body frame about the axis given by the integral of the component of the angular rate along the axis, as shown in eq. (3). Notice that Θ remains fixed during the time interval, T.

$$\int_0^T \omega(t)\cos(\theta)\,dt = \cos(\theta)\int_0^T \omega(t)\,dt = \lambda\cos(\theta) \tag{3}$$

If the rotational transformation occurs before the slewing transformation, the rotational transformation is obtained by a rotation of λ cos(Θ) about the axis at orientation **A**, as given in eq. (4).

$$\mathbf{U_R} = \mathbf{R}[\mathbf{A},\ \lambda\cos(\theta)] \tag{4}$$

If the slewing transformation occurs before the rotational transformation, the rotational transformation is performed when the axis is at orientation **B**, shown in eq. (5).

$$\mathbf{U_R} = \mathbf{R}[\mathbf{B},\ \lambda\cos(\theta)] \tag{5}$$

The rotational transformation in eq. (4) is not equal to the transformation in eq. (5), since the rotations are about different axis orientations. The total transformation is the product of the slewing and rotational transformation rotations, as expressed in eq. (6).

$$\mathbf{U} = \mathbf{R}(\boldsymbol{z},\ \lambda) = \mathbf{U_S}\,\mathbf{U_R} = \mathbf{U_S}\,\mathbf{R}[\mathbf{B},\ \lambda\cos(\theta)] \tag{6}$$

An earlier work (Patera, 2020a) established that the slewing and rotational transformations commute as long as the slewing trajectory is fixed in the inertial frame and the axis of the rotational transformation is accounted for. Therefore, the total transformation can also be expressed as eq. (7), where the rotation of the body frame is about the axis at orientation **A**, which occurs prior to the slewing transformation.

$$\mathbf{U} = \mathbf{R}(\mathbf{z},\ \lambda) = \mathbf{R}[\mathbf{A},\ \lambda\cos(\theta)]\ \mathbf{U_S} \tag{7}$$

The slewing transformation can be obtained by multiplying the inverse of the rotational transformation from eq. (5) by both sides of eq. (6) to obtain eq. (8).

$$\mathbf{U_S} = \mathbf{R}(\mathbf{z},\lambda)\ \mathbf{R^{-1}}[\mathbf{B},\lambda\ cos(\theta)] = \mathbf{R}(\mathbf{z},\ \lambda)\ \mathbf{R}[\mathbf{B},-\lambda\ cos(\theta)] \tag{8}$$

The inverse of the rotational transformation about **B** on the right hand side of eq. (8) is represented by the negative of the rotation angle. Since the transformations in eq. (8) commute, the slewing transformation can also be expressed as in eq. (9), with the rotation about axis **A** instead of axis B. Eq. (9) can also be obtained by multiplying eq. (7) by the inverse of eq. (4).

$$\mathbf{U_S} = \mathbf{R}[\mathbf{A},-\lambda\cos(\theta)]\ \mathbf{R}(\mathbf{z},\ \lambda) \tag{9}$$

If the axis slews one complete revolution about the **z**-axis, λ = 2π in eq. (8) and the slewing transformation is equivalent to a rotation of -2π cos(Θ) or 2π [1-cos(Θ)] about the axis, as shown in eq. (10). Note that **R(z,** 2π) equals the identity matrix in eq. (10).

$$\mathbf{U_S} = \mathbf{R}[\mathbf{A},-2\pi\cos(\theta)]\ \mathbf{R}(\mathbf{z},2\pi) = \mathbf{R}\{\mathbf{A},2\pi[1-\cos(\theta)]\} \tag{10}$$

This is in agreement with Ishlinskii's Theorem [Ishlinskii, 1952], which states that after one complete revolution, the resulting rotation angle about the axis is the solid angle enclosed by the slewing motion of the axis, as given in eq. (11).

$$\Omega = 2\pi\ [1-\cos(\theta)] \tag{11}$$

It should be noted that the slewing transformations derived in eqs. (8) and (9) are highly accurate, since they contain only associated numerical error.

The slewing transformations of eqs. (8) and (9) have already found application in developing the kinematics of the Foucault Pendulum [Patera, 2020b] and in deriving the precessional motion of the pendulum.

3. Algorithm derivation for a changing angular rate vector direction

Attitude propagation for a body frame with respect to the inertial frame is achieved by using a single axis that is fixed in the inertial frame. This axis slews in the body frame, as it is driven by the angular rate vector while the body rotates about the axis due to the component of the angular rate along the axis. Thus, the total attitude transformation is the product of the slewing transformation of an axis in the body frame and the rotational transformation of the body about the axis over the propagation time interval. It is assumed that both the angular rate vector and its slew rate vector are provided as input to the algorithm. Since an earlier work provided several methods to obtain the slew rate vector from the time dependent angular rate vector [Patera, 2010], those methods will not be included in this work. The slew rate vector of the slewing angular rate vector is assumed to be in a fixed direction in the body frame, which is a valid assumption for sufficiently short propagation intervals, as well as, pure coning motion over long time intervals. In addition, it is assumed that the slew rate vector has a time dependent magnitude proportional to the time dependent magnitude of the angular rate vector throughout the propagation time interval. Although the axis is fixed in the inertial frame, it slews in the body frame, because it is driven by the angular rate vector. The initial orientation of the axis in the body frame is selected, such that it slews at the same rate as the angular rate vector itself. This condition remains valid throughout each propagation time interval and enables the slewing transformation to be accurately computed. The rotational transformation is then computed based on the integral of the angular rate along the axis during the propagation interval. The total transformation is the product of the slewing and rotational transformations and can be expressed with two equivalent equations due to the commutative property of the slewing and rotational transformations.

Assume that the angular rate vector makes an angle of Θ with respect to the **z**-axis and slews in the counterclockwise direction about the **z**-axis, as given in eq. (12), where ϕ is a function of time.

$$\boldsymbol{\omega} = \begin{bmatrix} \omega \sin(\theta) \cos(\phi) \\ \omega \sin(\theta) \sin(\phi) \\ \omega \cos(\theta) \end{bmatrix} \tag{12}$$

Assume that the axis makes an angle of ϵ with respect to the **z**-axis and slews about the z-axis in unison with the angular rate, as shown in eq. (13).

$$\mathbf{A} = \begin{bmatrix} \sin(\epsilon) \cos(\phi) \\ \sin(\epsilon) \sin(\phi) \\ \cos(\epsilon) \end{bmatrix} \tag{13}$$

Since **A** is driven by the angular rate vector, its rate of change in the body frame is given by **A** x **ω**, as shown in eq. (14).

$$\frac{\boldsymbol{dA}}{\boldsymbol{dt}} = \mathbf{A}\ x\ \boldsymbol{\omega} = \begin{bmatrix} -\omega \sin(\phi) \sin(\theta - \epsilon) \\ \omega \cos(\phi) \cos(\theta - \epsilon) \\ 0 \end{bmatrix} \tag{14}$$

The change in **A** can also be found by taking the time derivative of eq. (13), as shown in eq. (15).

$$\frac{\boldsymbol{dA}}{\boldsymbol{dt}} = \begin{bmatrix} -\alpha \sin(\epsilon) \sin(\phi) \\ \alpha \sin(\epsilon)\, cos(\phi) \\ 0 \end{bmatrix}, \qquad \text{where} \quad \alpha = \frac{d\phi}{dt} \tag{15}$$

Equating the rate of change of the components of **A** from eqs. (14) and (15) provides the orientation of **A** by yielding ϵ, as shown in eq. (16).

$$\epsilon = tan^{-1}\left[\frac{\omega \sin(\theta)}{\alpha + \omega \cos(\theta)}\right] \tag{16}$$

An important feature of eq. (16) is that ϵ does not change as long as the magnitude of **α** is proportional to the magnitude of **ω**, even when both α and ω are time dependent. When eq. (16) holds, attitude can be propagated without error for time varying α and ω.

Fig. 2 is created by using the numerator and denominator of the argument in eq. (16) and shows that the axis, **A**, is directed parallel to **α + ω**. The x and z components of **α** + **ω** are ω sin(Θ) and α + ω cos(Θ), respectively. The hypotenuse, ψ, in Fig. 2 equals the magnitude of **α + ω** and can be expressed as shown in eq. (17), since the angle between **A** and **α** is ϵ and the angle between **A** and **ω** is Θ - ϵ.

$$\psi = |\boldsymbol{\alpha} + \boldsymbol{\omega}| = (\boldsymbol{\alpha} + \boldsymbol{\omega}) \cdot \mathbf{A} = \alpha \cos(\epsilon) + \omega \cos(\theta - \epsilon) \tag{17}$$

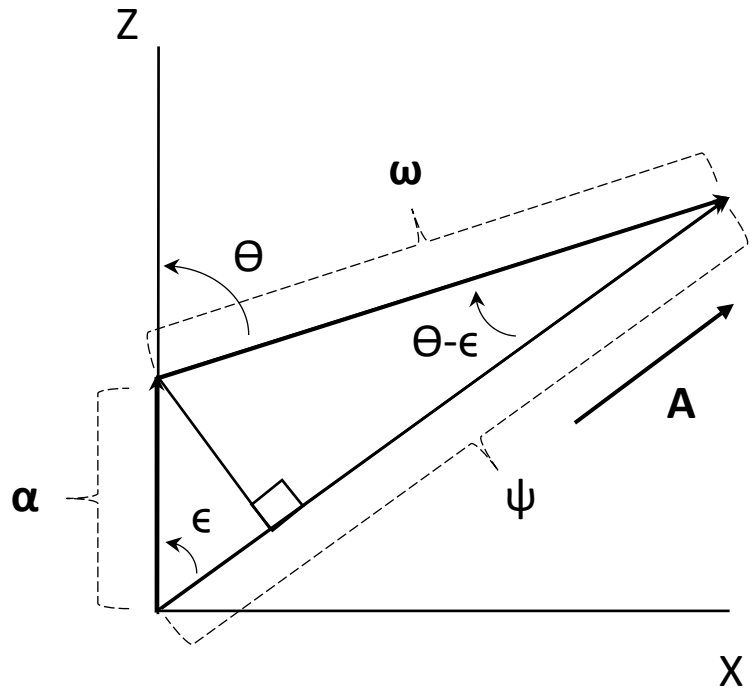

Fig. 2 Axis **A** is shown to be parallel to **α** + **ω**, which has magnitude ψ.

When the axis is oriented with angle, ϵ, from eq. (16), the angular rate vector drives the axis in the body frame, such that it slews about the **z**-axis with rate **α**, and maintains a constant angular separation from the **z**-axis. At the initial time, t=0, the **z**-axis, **A** and **ω** all are contained in the same plane, as shown in Fig. 3. The slewing axis, **A**, maintains angle ϵ with the z-axis and angle (Θ - ϵ) with **ω** throughout the propagation interval.

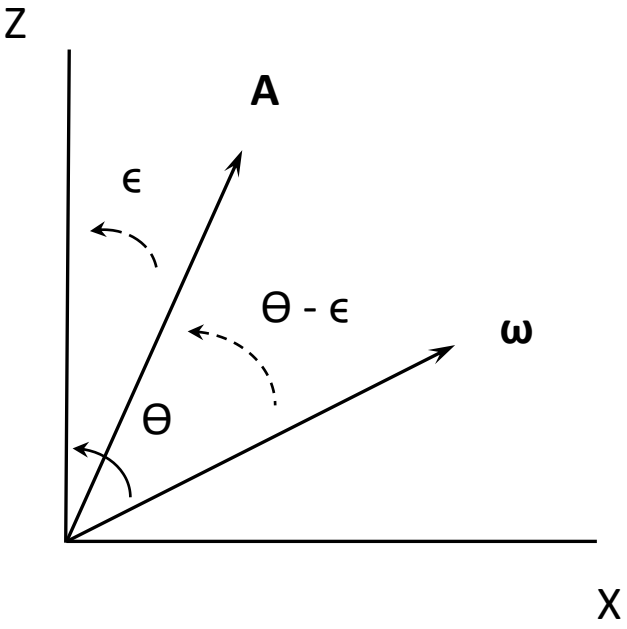

Fig. 3 Relative angular separations among **A**, **ω** and the z-axis during the propagation interval.

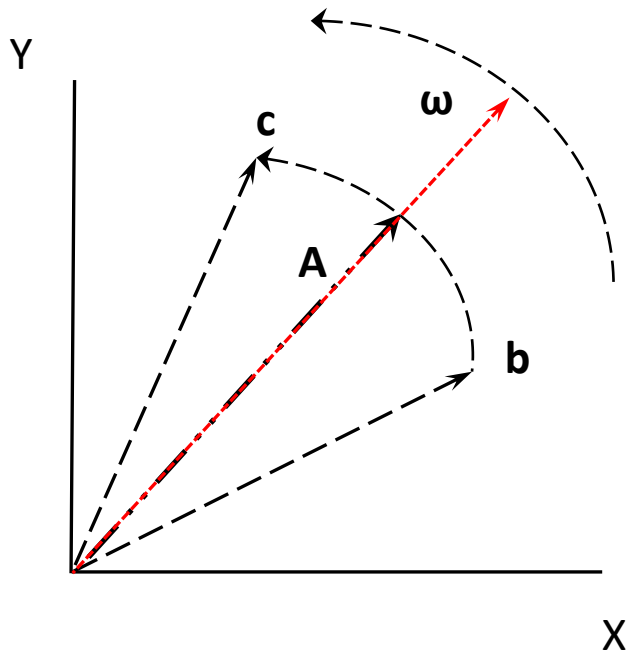

Fig. 4 Slewing arcs of **A** and **ω**, as **A** moves from orientation **b** to orientation **c**.

Fig. (4) illustrates the slewing motion of both the angular rate vector and the axis, **A**, about the slew rate vector, **α**, which is directed out of the page along the z-axis. Point **b** is the location of the tip of the axis at t=0, and point **c** is the location of the tip of the axis at the end of the propagation time interval, T. The total attitude transformation involves the slewing transformation of the axis, as its tip moves from point **b** to point **c** in Fig. 4 and the rotational transformation of the body frame about the axis during the propagation time interval. Although the axis slews because it is driven by **ω**, its slewing motion is exactly the same as if it were driven by **α**. Therefore, **α** is used to slew **A**, since it results in error free slewing propagation, whereas, slewing **A** using **ω** results in coning error. Coning error is caused by the changing direction of **ω**. Since **α** maintains a fixed orientation in the body frame, it does not suffer coning error. The slewing transformation of the axis is given by eq. (18), where **k** is the unit vector directed along the z-axis, and Ω is slew angle defined in eq. (19). Eq. (18) is in similar form to eq. (9) except that the associated angles change sign, since they reference body to inertial rather that inertial to body transformations referenced by eq. (9). The slewing transformation in eq. (18) represents the transformation of the body frame to the inertial frame.

$$\mathbf{U_S} = \mathbf{R}(\mathbf{k}, -\Omega)\,\mathbf{R}[\mathbf{c}, \Omega\cos(\epsilon)] = \mathbf{R}[\mathbf{b}, \Omega\cos(\epsilon)]\,\mathbf{R}(\mathbf{k}, -\Omega) \tag{18}$$

$$\Omega = \int_0^T \alpha\, dt \tag{19}$$

The first term on the right hand side of eq. (18) is a rotation about the **z**-axis of -Ω followed by a rotation about the axis at orientation **c** of Ω cos(ϵ). The rotation about the axis at orientation **c** ensures that the motion is purely slewing motion and does not involve rotation about the axis itself. The second method of representing the slewing transformation is given by the final two terms in eq. (18). The first term is a rotation about the axis at orientation **b** to ensure the motion is purely slewing motion and does not involve rotation about the axis itself. The last term is a rotation about the **z**-axis of -Ω, which slews the axis from orientation **b** to orientation **c** in the body frame. The two different representations in eq. (18) are possible due to the commutation property of slewing and rotational transformations, that was developed in an earlier work [Patera, 2020a]. Note that although rotational transformations are used in eq. (18), the transformation, $\mathbf{U_S}$ is a pure slewing transformation of the body frame.

The axis appears to slew from orientation **b** to orientation **c** in the body frame, as the body frame slews according to $\mathbf{U}_S$.

The rotational part of the total transformation is the integral of the component of the angular rate vector that is parallel to the axis. The angle between **A** and **ω** is Θ - ϵ, which remains fixed throughout the propagation interval, so that the rotation angle about the axis can be easily computed, as shown in eq. (20), where λ is the integral of the angular rate magnitude.

$$\cos(\Theta - \epsilon) \int_0^T \omega(t)\, dt = \lambda \cos(\Theta - \epsilon) \tag{20}$$

One can apply the rotation along the axis at orientation **b** from eq. (20) and combine it with the slewing transformation, $\mathbf{U}_S$ from eq. (18) to obtain the total transformation, given in eq. (21).

$$\mathbf{U} = \mathbf{R}[\mathbf{b}, \lambda \cos(\Theta - \epsilon)]\, \mathbf{U_S} = \mathbf{R}[\mathbf{b}, \lambda \cos(\Theta - \epsilon)]\, \mathbf{R}[\mathbf{b}, \Omega \cos(\epsilon)]\, \mathbf{R}(\mathbf{k}, -\Omega) \tag{21}$$

The two rotations about the axis at orientation **b** can be combined, since they are about the same axis direction, as shown in eq. (22).

$$\mathbf{U} = \mathbf{R}[\mathbf{b}, \Omega \cos(\epsilon) + \lambda \cos(\Theta - \epsilon)]\, \mathbf{R}(\mathbf{k}, -\Omega) \tag{22}$$

Alternatively, the slewing transformation can be applied first and the rotational transformation can be applied about the axis at orientation **c**, as illustrated in eq. (23).

$$\mathbf{U} = \mathbf{R}(\mathbf{k}, -\Omega)\, \mathbf{R}[\mathbf{c}, \Omega \cos(\epsilon) + \lambda \cos(\Theta - \epsilon)] \tag{23}$$

Eqs. (22) and (23) can be simplified by noting that the rotation angle about the axis at either orientation **b** or orientation **c** is given by eq. (24), which is the integral of the angular rate given in eq. (17).

$$\Delta = \int_0^T \psi\, dt = \int_0^T |\boldsymbol{\alpha} + \boldsymbol{\omega}| dt = \int_0^T [\alpha \cos(\epsilon) + \omega \cos(\Theta - \epsilon)]\, dt = \Omega \cos(\epsilon) + \lambda \cos(\Theta - \epsilon) \tag{24}$$

Therefore, eqs. (22) and (23) can be written compactly as eqs. (25) and (26).

$$\mathbf{U} = \mathbf{R}(\mathbf{b}, \Delta)\, \boldsymbol{R}(\mathbf{k}, -\Omega) \tag{25}$$

$$\mathbf{U} = \mathbf{R}(\mathbf{k}, -\Omega)\, \mathbf{R}(\mathbf{c}, \Delta) \tag{26}$$

The new results given by eqs. (25) and (26) are valid for time varying **α** and **ω**, when the magnitude of **α** is proportional to the magnitude of **ω**. When both **α** and **ω** are constant, eq. (25) is consistent with an earlier published result [Patera, 2010] and when the magnitudes of **α** and **ω** are proportional, eq. (25) is equivalent to an earlier result [Patera, 2011]. Eq. (6) is a new result obtained from the current work.

4. Propagating the attitude of axisymmetric vehicles

The attitude propagation method developed in Section 3 is directly applicable to axisymmetric spinning vehicles with no external torque. In this case, the angular rate vector slews about the symmetric axis and drives the angular momentum vector, which is constant in the inertial frame during the propagation interval.
Let the angular rate vector make an angle of Θ with the spin axis or z-axis and let the spin and transverse moment of inertias be I_S and I_T, respectively. The angular momentum, **J**, is given by eq. (27), where Θ and ϕ are standard polar coordinates.

$$\mathbf{J} = \mathbf{I} \cdot \boldsymbol{\omega} = \begin{pmatrix} I_T & 0 & 0 \\ 0 & I_T & 0 \\ 0 & 0 & I_S \end{pmatrix} \begin{bmatrix} \omega \sin(\Theta) \cos(\phi) \\ \omega \sin(\Theta) \sin(\phi) \\ \omega \cos(\Theta) \end{bmatrix} = \begin{bmatrix} I_T\, \omega \sin(\Theta) \cos(\phi) \\ I_T\, \omega \sin(\Theta) \sin(\phi) \\ I_S\, \omega \cos(\Theta) \end{bmatrix} \tag{27}$$

Since, the angular momentum vector is fixed in inertial space, it takes the role of the axis, **A**, in Section 3. Therefore, the angle, ϵ, between **J** and the z-axis is obtained from eq. (28).

$$\tan(\epsilon) = \frac{J_T}{J_S} = \frac{\omega \sin(\theta)\, I_T}{\omega \cos(\theta)\, I_S} = \frac{I_T}{I_S} \tan(\theta) \tag{28}$$

The magnitude of the slew rate, α, can be obtained by equating eq. (28) with tan(ϵ) obtained from eq. (16) in Section 3, as shown in eq. (29).

$$\tan(\epsilon) = \left[\frac{\omega \sin(\theta)}{\alpha + \omega \cos(\theta)}\right] = \left[\frac{\sin(\theta)\, I_T}{\cos(\theta)\, I_S}\right] \tag{29}$$

Solving for α in eq. (29), one finds that the slew rate magnitude is proportional to the angular rate magnitude, which maintains a constant value of ϵ in eq. (29) throughout the propagation interval, as shown in eq. (30). Notice that α is in the opposite direction of ω, if I_S is less than I_T in eq. (30).

$$\alpha = \omega \cos(\theta) \left(\frac{I_S}{I_T} - 1\right) \tag{30}$$

Since **α**, is directed along the z-axis, it is given by eq. (31).

$$\boldsymbol{\alpha} = \begin{bmatrix} 0 \\ 0 \\ \omega \cos(\theta) \left(\frac{I_S}{I_T} - 1\right) \end{bmatrix} \tag{31}$$

Using **ω** from eq. (27) and **α** from eq. (31), one finds that **α** + **ω** makes an angle of ϵ with respect to the z-axis, as shown in eq. (32).

$$\boldsymbol{\alpha} + \boldsymbol{\omega} = \begin{bmatrix} \omega \sin(\theta) \cos(\phi) \\ \omega \sin(\theta) \sin(\phi) \\ \omega \frac{I_S}{I_T} \cos(\theta) \end{bmatrix} = \frac{\boldsymbol{J}}{I_T} = \frac{J}{I_T} \begin{bmatrix} \sin(\epsilon) \cos(\phi) \\ \sin(\epsilon) \sin(\phi) \\ \cos(\epsilon) \end{bmatrix} \tag{32}$$

The definitions of Ω, λ and Δ remain the same as in Section 3, as shown in eqs. (33) and (34). Since **α** is along the z-axis, its integral, Ω, is equal to ϕ that appears in eq. (27), since ϕ = 0 at t = 0.

$$\Omega = \int_0^T \alpha \, dt \qquad\qquad \lambda = \int_0^T \omega(t) \, dt \tag{33}$$

Using eq. (30) in eq. (33), one obtains eq. (34).

$$\Omega = \lambda \cos(\theta) \left(\frac{I_S}{I_T} - 1\right) \tag{34}$$

The rotation angle given by eq. (35) can be reduced to eq. (36), by using eq. (27).

$$\Delta = \int_0^T [\alpha \cos(\epsilon) + \omega \cos(\theta - \epsilon)] \, dt = \Omega \cos(\epsilon) + \lambda \cos(\theta - \epsilon) = \int_0^T |\boldsymbol{\alpha} + \boldsymbol{\omega}| \, dt \tag{35}$$

$$\Delta = \int_0^T |\boldsymbol{\alpha} + \boldsymbol{\omega}| dt = \lambda \sqrt{\sin(\theta)^2 + \left[\left(\frac{I_S}{I_T}\right)^2 \cos(\theta)^2\right]} \tag{36}$$

The attitude transformations from Section 3 are also valid, as shown in eqs. (37) and (38), where **b** and **c** are the initial and final orientations of **J** in the body frame. Eq. (27) and (29) can be used to obtain the unit vectors **b** and **c**, as shown in eqs. (39) and (40).

$$\mathbf{U} = \mathbf{R}(\mathbf{b}, \Delta)\ \boldsymbol{R}(\mathbf{k}, -\Omega) \tag{37}$$

$$\mathbf{U} = \mathbf{R}(\mathbf{k}, -\Omega)\ \mathbf{R}(\mathbf{c}, \Delta) \tag{38}$$

$$\mathbf{J}(\mathbf{0}) = \begin{bmatrix} I_T\ \omega \sin(\theta) \\ 0 \\ I_S\ \omega \cos(\theta) \end{bmatrix}, \qquad \mathbf{J}(\mathbf{T}) = \begin{bmatrix} I_T\ \omega \sin(\theta) \cos(\Omega) \\ I_T\ \omega \sin(\theta) \sin(\Omega) \\ I_S\ \omega \cos(\theta) \end{bmatrix} \tag{39}$$

$$\mathbf{b} = \frac{\mathbf{J(0)}}{J} = \begin{bmatrix} \sin(\epsilon) \\ 0 \\ \cos(\epsilon) \end{bmatrix}, \qquad \mathbf{c} = \frac{\mathbf{J(T)}}{\mathrm{J}} = \begin{bmatrix} \sin(\epsilon) \cos(\Omega) \\ \sin(\epsilon) \sin(\Omega) \\ \cos(\epsilon) \end{bmatrix} \tag{40}$$

The attitude propagation solutions developed in eq. (37) and eq. (38) are valid for time dependent angular rate magnitude, since the slew rate magnitude is proportional to the angular rate magnitude, as shown in eq. (30).

One can represent the rotations in eq. (37) as Pivot Parameters [Patera, 2017], with each rotation having two associated Pivot Vectors, as shown in eqs. (41) and (42), where $\mathbf{V_3}$ is directed along the negative y-axis. Each transformation is equivalent to 180 degree rotations about the associated Pivot Vectors. The product of the transformations is given in eq. (43), where the 180 degree rotations about $\mathbf{V_3}$ cancel and reduce to no rotation.

$$\mathbf{R}(\mathbf{b}, \Delta) = \mathbf{R}(\mathbf{V_1}, 180)\ \mathbf{R}(\mathbf{V_3}, 180) \tag{41}$$

$$\mathbf{R}(\mathbf{k}, -\Omega) = \mathbf{R}(\mathbf{V_3}, 180)\ \mathbf{R}(\mathbf{V_2}, 180) \tag{42}$$

$$\mathbf{U} = \mathbf{R}(\mathbf{V_1}, 180)\ \mathbf{R}(\mathbf{V_3}, 180)\ \mathbf{R}(\mathbf{V_3}, 180)\ \mathbf{R}(\mathbf{V_2}, 180) = \mathbf{R}(\mathbf{V_1}, 180)\mathbf{R}(\mathbf{V_2}, 180) \tag{43}$$

The values of $\mathbf{V_1}$, $\mathbf{V_2}$, and $\mathbf{V_3}$ are given in eqs. (44) – (46).

$$\mathbf{V_1} = \begin{bmatrix} \sin\left(\frac{\Delta}{2}\right) cos(\epsilon) \\ -\cos\left(\frac{\Delta}{2}\right) \\ -\sin\left(\frac{\Delta}{2}\right) \sin(\epsilon) \end{bmatrix} \tag{44}$$

$$\mathbf{V_2} = \begin{bmatrix} \sin\left(\frac{\Omega}{2}\right) \\ -cos\left(\frac{\Omega}{2}\right) \\ 0 \end{bmatrix} \tag{45}$$

$$\mathbf{V_3} = \begin{pmatrix} 0 \\ -1 \\ 0 \end{pmatrix} \tag{46}$$

The associated quaternion is found by the cross product and dot product [Patera, 2017], shown in eqs. (47) and (48), respectively.

$$\mathbf{q} = \mathbf{V_2} \times \mathbf{V_1} = \begin{bmatrix} \cos\left(\frac{\Omega}{2}\right)\sin\left(\frac{\Delta}{2}\right)\sin(\epsilon) \\ \sin\left(\frac{\Omega}{2}\right)\sin\left(\frac{\Delta}{2}\right)\sin(\epsilon) \\ \cos\left(\frac{\Omega}{2}\right)sin\left(\frac{\Delta}{2}\right)\cos(\epsilon) - \sin\left(\frac{\Omega}{2}\right)\cos\left(\frac{\Delta}{2}\right) \end{bmatrix} \tag{47}$$

$$q_0 = \mathbf{V_1} \cdot \mathbf{V_2} = \cos\left(\frac{\Delta}{2}\right)\cos\left(\frac{\Omega}{2}\right) + \sin\left(\frac{\Omega}{2}\right)\sin\left(\frac{\Delta}{2}\right)\cos(\epsilon) \tag{48}$$

A similar analysis can be performed starting with eq. (38) instead of eq. (37) and the resulting transformation will be the same, since the transformation in eq. (37) is the same as that of eq. (38).

This development shows that once Ω, Δ, and ϵ are obtained, the total transformation is given by eq. (43) with Pivot Vectors in eqs. (44) and (45). The transformation is also represented by the quaternion given in eqs. (47) and (48).

5. Applying results to pure coning motion

The results in Section 3 can be applied to the case of pure coning motion, which involves the slewing angular rate vector given by eq. (49) with the time dependent slew rate given by eq. (50).

$$\boldsymbol{\omega} = \begin{bmatrix} \alpha\sin(\epsilon)\cos(\phi) \\ -\alpha\sin(\epsilon)\sin(\phi) \\ \alpha[1-\cos(\epsilon)] \end{bmatrix} \tag{49}$$

$$\boldsymbol{\alpha} = \begin{pmatrix} 0 \\ 0 \\ -\alpha \end{pmatrix} \tag{50}$$

Using eqs. (49) and (50), the magnitude of the slew rate was found to be proportional to the magnitude of the angular rate, as shown in eq. (51). The proportionality in eq. (51) permits attitude propagation without error for time varying α and ω, as was shown in Section 3.

$$\alpha = \frac{\omega}{\sqrt{2\,[1-\cos(\epsilon)]}} = \frac{\omega}{2\sin\left(\frac{\epsilon}{2}\right)} \tag{51}$$

Using the trigonometric identities in eq. (52), the angular rate in eq. (49) can be written, as shown in eq. (53) with the magnitude of **ω** obtained from eq. (51). Thus, the angular rate makes an angle of Θ with respect to the z-axis, where Θ = π/2 - ϵ/2.

$$\sin(\epsilon) = 2\sin\left(\frac{\epsilon}{2}\right)\cos\left(\frac{\epsilon}{2}\right), \qquad \left[\sin\left(\frac{\epsilon}{2}\right)\right]^2 = [1-\cos(\epsilon)]/2 \tag{52}$$

$$\boldsymbol{\omega} = \omega\begin{bmatrix} \cos\left(\frac{\epsilon}{2}\right)\cos(\phi) \\ -\cos\left(\frac{\epsilon}{2}\right)\sin(\phi) \\ \sin\left(\frac{\epsilon}{2}\right) \end{bmatrix} = \omega\begin{bmatrix} \sin(\theta)\cos(\phi) \\ -\sin(\theta)\sin(\phi) \\ \cos(\theta) \end{bmatrix} \tag{53}$$

The attitude can be propagated using eq. (25) or eq. (26) with Δ from eq. (24) and Ω from eq. (19). The unit vector, **b**, in eq. (25) is the value **A(t)** at t=0, which is parallel to **α** + **ω**, as was shown in Section 3. Using eqs. (49) and (50), one obtains rotational transformation rate vector, which makes an angle of ϵ with respect to the negative z-axis, as shown in eq. (54).

$$\boldsymbol{\alpha} + \boldsymbol{\omega} = \begin{bmatrix} \alpha \sin(\epsilon) \cos(\phi) \\ -\alpha \sin(\epsilon) \sin(\phi) \\ -\alpha \cos(\epsilon) \end{bmatrix} = \alpha \begin{bmatrix} \sin(\epsilon) \cos(\phi) \\ -\sin(\epsilon) \sin(\phi) \\ -\cos(\epsilon) \end{bmatrix} = \alpha\, \mathbf{A}(\mathbf{t}) \tag{54}$$

Therefore, **b** and Δ are found from eq. (54), as given in eq. (55).

$$\mathbf{b} = \mathbf{A}(\mathbf{0}) = \begin{bmatrix} \sin(\epsilon) \\ 0 \\ -\cos(\epsilon) \end{bmatrix};\ \Delta = \int_0^T \alpha\, dt \tag{55}$$

Using eq. (55), the rotational transformation from eq. (25) is given in eq. (56).

$$\mathbf{U_R} = \mathbf{R}(\mathbf{b}, \Delta) \tag{56}$$

Since the slew rate vector of the angular rate vector is along the negative z-axis, as shown in eq. (50), the slewing transformation is given by eq. (57).

$$\mathbf{R}(\mathbf{k}, -\Omega) = \mathbf{R}(\mathbf{k}, \Delta) \tag{57}$$

The combined transformation is the product of the rotational and slewing transformations, as given in eq. (58). If we perform the slewing transformation before the rotational transformation, as in eq. (26), the second solution is obtained in eq. (59), where **c** is defined in eq. (60).

$$\mathbf{U} = \mathbf{R}(\mathbf{b}, \Delta)\, \boldsymbol{R}(\mathbf{k}, -\Omega) = \boldsymbol{R}(\mathbf{b}, \Delta)\, \mathbf{R}(\mathbf{k}, \Delta) \tag{58}$$

$$\mathbf{U} = \mathbf{R}(\mathbf{k}, -\Omega)\, \boldsymbol{R}(\mathbf{c}, \Delta) = \boldsymbol{R}(\mathbf{k}, \Delta)\, \mathbf{R}(\mathbf{c}, \boldsymbol{\Delta}) \tag{59}$$

$$\mathbf{c} = \mathbf{A}(\mathbf{T}) = \begin{bmatrix} \sin(\epsilon)\cos(\Delta) \\ -\sin(\epsilon) \sin(\Delta) \\ -\cos(\epsilon) \end{bmatrix} \tag{60}$$

It should be noted that the attitude transformation due to pure coning motion given by eqs. (58) and (59) cannot be obtained with a realistic choice of inertia ratio, I_T/I_S, of an axisymmetric vehicle with no external torques. In the limiting unrealistic case, when the inertia ratio of an axisymmetric vehicle becomes very large, ϵ approaches 90 degrees, Θ approaches 45 degrees and the ratio of ω/α approaches $-\sqrt{2}$ for both pure coning motion and the axisymmetric vehicle. This case can never be realized because the transverse inertia, I_T, must be finite.

When **R**(**b**,Δ) and **R**(**k**,Δ) are represented as Pivot Vectors (Patera, 2017) and combined, the transformation in eq. (58) becomes eq. (61) with the Pivot Vectors defined in eq. (62).

$$\mathbf{U} = \mathbf{R}(\mathbf{V_1}, 180)\, \mathbf{R}(\mathbf{V_2}, 180) \tag{61}$$

$$\mathbf{V_1} = \begin{bmatrix} \sin\left(\frac{\Delta}{2}\right) \cos(\epsilon) \\ \cos\left(\frac{\Delta}{2}\right) \\ \sin\left(\frac{\Delta}{2}\right) \sin(\epsilon) \end{bmatrix}, \qquad \mathbf{V_2} = \begin{bmatrix} \sin\left(\frac{\Delta}{2}\right) \\ \cos\left(\frac{\Delta}{2}\right) \\ 0 \end{bmatrix} \tag{62}$$

Since Pivot Vectors are not unique, the transformation in eq. (61) can also be represented by the Pivot Vector pair, $\mathbf{V_3}$, $\mathbf{V_4}$, which has time dependance in $\mathbf{V_4}$ but not in $\mathbf{V_3}$, as shown in eq. (63).

$$\mathbf{U} = \mathbf{R}(\mathbf{V_3}, 180)\, \mathbf{R}(\mathbf{V_4}, 180), \qquad \mathbf{V_3} = \begin{pmatrix} -\sin\left(\frac{\epsilon}{2}\right) \\ 0 \\ \cos\left(\frac{\epsilon}{2}\right) \end{pmatrix}, \qquad \mathbf{V_4} = \begin{bmatrix} -\sin\left(\frac{\epsilon}{2}\right) \cos(\Delta) \\ \sin\left(\frac{\epsilon}{2}\right) \sin(\Delta) \\ \cos\left(\frac{\epsilon}{2}\right) \end{bmatrix} \tag{63}$$

Eqs. (58), (59), (61) and (63) represent the attitude propagation solution for pure coning motion associated with eqs. (49) and (50).

The total attitude solution for pure coning motion reported in various publications (Bortz, 1971; Patera, 2010) includes the initial tilt angle of ϵ degrees about the y-axis. Therefore, with the addition of the tilt angle, eqs.(58) and (59) become eqs. (64) and (65), respectively.

$$\mathbf{U_T} = \mathbf{R}(\mathbf{j}, \epsilon)\, \mathbf{U} = \mathbf{R}(\mathbf{j}, \epsilon)\, \mathbf{R}(\mathbf{b}, \Delta)\, \mathbf{R}(\mathbf{k}, \Delta) \tag{64}$$

$$\mathbf{U_T} = \mathbf{R}(\mathbf{j}, \epsilon)\, \mathbf{U} = \mathbf{R}(\mathbf{j}, \epsilon)\, \mathbf{R}(\mathbf{k}, \Delta)\, \mathbf{R}(\mathbf{c}, \Delta) \tag{65}$$

If the initial tilt angle can be represented by the Pivot Vectors in eq. (66), the total transformation can be obtained from eq. (63) and (66), as shown in eq. (67). The two 180 degree rotations about $\mathbf{V_3}$ result in no rotation, which reduces eq. (67) to eq. (68).

$$\mathbf{R}(\mathbf{j}, \Delta) = \mathbf{R}(\mathbf{V_5}, 180)\, \mathbf{R}(\mathbf{V_3}, 180)\,, \qquad \mathbf{V_5} = \begin{pmatrix} 0 \\ 0 \\ 1 \end{pmatrix} \tag{66}$$

$$\mathbf{U_T} = \mathbf{R}(\mathbf{j}, \boldsymbol{\epsilon})\, \mathbf{U} = \mathbf{R}(\mathbf{V_5}, 180)\, \mathbf{R}(\boldsymbol{V_3}, 180)\, \mathbf{R}(\mathbf{V_3}, 180)\, \mathbf{R}(\mathbf{V_4}, 180) \tag{67}$$

$$\mathbf{U_T} = \mathbf{R}(\mathbf{V_5}, 180)\, \mathbf{R}(\mathbf{V_4}, 180) = \begin{pmatrix} 0 \\ 0 \\ 1 \end{pmatrix} \begin{bmatrix} -\sin\left(\frac{\epsilon}{2}\right) \cos(\Delta) \\ sin\left(\frac{\epsilon}{2}\right) \sin(\Delta) \\ cos\left(\frac{\epsilon}{2}\right) \end{bmatrix} \tag{68}$$

Therefore, the total transformation in eqs. (64) and (65) reduce to two 180 degree rotations given in eq. (68), which is in agreement with published results (Patera, 2017) obtained using a different method.

The associated quaternion (Patera, 2017) and Euler Vector (Bortz, 1971) representations of $\mathbf{U_T}$ are shown in eq. (69) and (70), respectively.

$$\mathbf{q} = \begin{bmatrix} \sin\left(\frac{\epsilon}{2}\right) \sin(\Delta) \\ \sin\left(\frac{\epsilon}{2}\right) \cos(\Delta) \\ 0 \end{bmatrix}, \quad q_0 = \cos\left(\frac{\epsilon}{2}\right) \tag{69}$$

$$\mathbf{\Phi} = \begin{bmatrix} \epsilon \sin(\Delta) \\ \epsilon \cos(\Delta) \\ 0 \end{bmatrix} \tag{70}$$

Thus, by including the initial tilt angle in the total transformation, $\mathbf{U_T}$, the associated Pivot Vectors, quaternion and Euler Vector have the simple expressions shown in eqs. (68) - (70).

6. Numerical results for a fixed angular rate vector orientation

The first numerical example involves computing the slewing transformation of an axis, **A,** having an orientation defined by standard polar coordinates, Θ and ϕ. The angular rate vector, **ω**, is aligned with the **z**-axis and can have a time dependent magnitude over the propagation time interval. The angular rate tangent to the axis is given by eq. (71) and the angular rate normal to the axis is given by eq. (72), where Θ is constant. In this example, ω is assumed to grow linearly, as given by eq. (73), however, other time dependences can be treated in a similar fashion. Since ϕ is the integral of ω over time, it is given by eq. (74).

$$\boldsymbol{\omega_T} = (\mathbf{A} \cdot \boldsymbol{\omega})\,\mathbf{A} = \begin{bmatrix} \omega \cos(\theta) \sin(\theta)\, cos(\phi) \\ \omega \cos(\theta) \sin(\theta) \sin(\phi) \\ \omega\, cos^2(\theta) \end{bmatrix} \tag{71}$$

$$\boldsymbol{\omega_N} = \boldsymbol{\omega} - \boldsymbol{\omega_T} = \begin{bmatrix} -\omega \cos(\theta) \sin(\theta)\, cos(\phi) \\ -\omega \cos(\theta) \sin(\theta) \sin(\phi) \\ \omega\, sin^2(\theta) \end{bmatrix} \tag{72}$$

$$\omega = \omega_0 + \omega_1\, t \tag{73}$$

$$\phi = \omega_0\, t + \omega_1\, t^2/2 \tag{74}$$

The angular rate vector is assumed to be constant over the time step, Δt, and a sequence of Euler Vector increments and associated transformations were created using the angular rate normal to the axis, as given in eq. (75).

$$\boldsymbol{\Delta\Theta_i} = \boldsymbol{\omega_i}\, \Delta t\ , \qquad \mathbf{R}(\boldsymbol{\Delta\Theta_i}, \Delta\Theta_i) \tag{75}$$

The total slewing transformation is the product of the incremental transformations, as shown in eq. (76).

$$\mathbf{U_S} = \prod_i \mathbf{R}(\boldsymbol{\Delta\Theta_i}, \Delta\Theta_i) \tag{76}$$

A computer simulation was created and used to determine the slewing transformation using the angular rate vector from eq. (72) with time dependent ω and ϕ given by eqs. (73) and (74), respectively. The slewing transformation was evaluated using eqs. (75) and (76). The error resulting from eq. (76) is essentially the same as that obtained by attitude propagation algorithms employing other attitude representations, such as Euler Angles, Quaternions, etc.

The slewing transformation was also computed using eqs. (18) and (19 with α, Ω, and ϵ replaced by ω, ϕ, and Θ, respectively, as shown in eqs. (77) and (78).

$$\mathbf{U_S} = \mathbf{R}(\mathbf{k}, -\phi)\, \mathbf{R}[\mathbf{c}, \phi \cos(\theta)] = \mathbf{R}[\mathbf{b}, \phi \cos(\theta)]\, \mathbf{R}(\mathbf{k}, -\phi) \tag{77}$$

$$\phi = \int_0^T \omega\, dt = \phi(T) - \phi(0) \tag{78}$$

The difference between results obtained from eq. (76) and eq. (77) was parameterized as a Euler Vector. The growth rate of magnitude of the Euler vector for each case in Table 1 was plotted on a logarithmic scale in Fig. 5. Since the results obtained from eq. (77) have no error other than numerical processing error, the error growth rate shown in Fig. 5 is due to propagation error associated with eq. (76). Results shown in Fig. 5 indicated that accuracy within each case is increased by decreasing the time step or increasing the propagation frequency in eq. (76), but the residual coning error growth rate is still present. It is clear that eq. (77) achieves a slewing transformation more accurately than the standard method of propagation used in eq. (76).

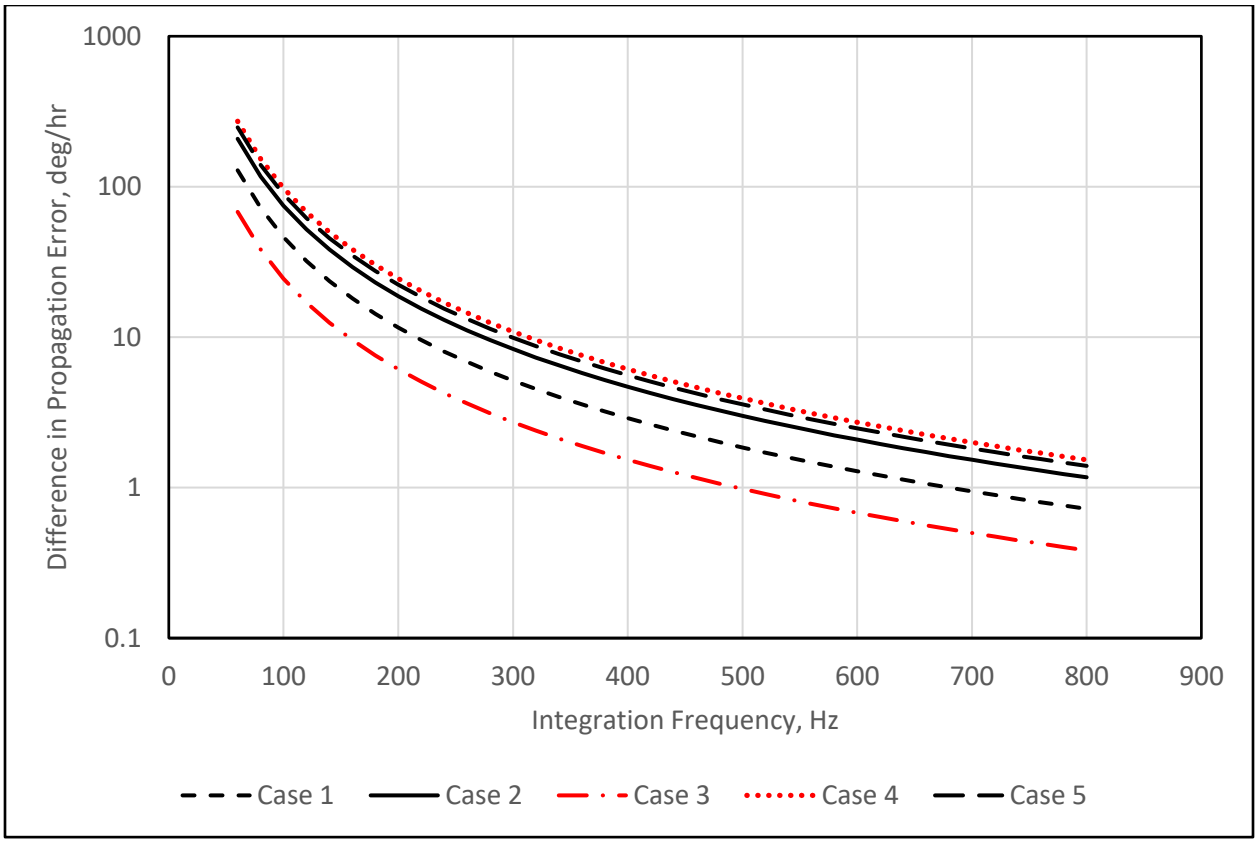

Fig. 5 Difference in propagation error between the new method and a standard method as a function of the integration frequency for the slewing transformation of the cases given in Table 1.

Table 1

Case #	Time, sec	Theta, deg.	ω_0	ω_1
1	100	60	300	0
2	100	60	300	1
3	80	50	200	1
4	60	30	400	2
5	40	20	500	3

7. Numerical results for axisymmetric vehicles

The general attitude propagation problem can be solved by dividing the propagation interval into subintervals with each having its angular rate vector slewing about a fixed axis in the body frame. The method of Section 3 can be applied to obtain each incremental attitude transformation, once the slewing motion of the angular rate vector is quantified by the slew angular rate vector, $\boldsymbol{\alpha}$. The product of the incremental transformations yields the total attitude transformation over the desired propagation time interval.

The slew angular rate vector for an axisymmetric vehicle with no external torque is the same for all the subintervals, so dividing the propagation time interval into subintervals is not necessary. The validity of the methods developed in Sections 2 and Section 3 can be achieved by propagating the attitude of an axisymmetric vehicle, where the slew rate of the angular rate is proportional to the magnitude of the angular rate vector. For

this case, the attitude can be propagated with essentially no error, even if the angular rate magnitude is time dependent.

Several cases involving various values of spin axis inertia, transverse axis inertia, initial angular rate vector angle with respect to the symmetric axis, and time dependent angular rate magnitude are included in Table 2. The functional form of the angular rate vector magnitude has a linear growth term and an oscillatory term as is shown in eq. (79). Since ϕ is the integral of ω over time, it is given by eq. (80).

$$\omega = \omega_0 + \omega_1 t + \omega_2 \sin(\omega_3 t) \tag{79}$$

$$\phi = \omega_0 t + \frac{1}{2}\omega_1 t^2 + \frac{\omega_2}{\omega_3}[1 - \cos(\omega_3 t)] \tag{80}$$

The attitude was propagated using the methods of Section 3 and Section 4, which are summarized in eqs. (37) and (38). The attitude was also propagated by creating incremental Euler Vectors from the angular rate vector and combining the associated attitude transformations to obtain the total attitude transformation, as shown in eqs. (81) and (82).

$$\mathbf{\Delta\theta_i} = \boldsymbol{\omega_i}\,\Delta t\,, \quad \mathbf{R}(\mathbf{\Delta\theta_i}, \Delta\theta_i) \tag{81}$$

$$\mathbf{U} = \prod_i \mathbf{R}(\mathbf{\Delta\theta_i}, \Delta\theta_i) \tag{82}$$

For each case in Table 2, the attitude was propagated for 40 seconds and the difference in attitude propagation using the proposed method and the standard method was quantified by a Euler Rotation Vector. The growth rate of the magnitude of the Euler Rotation vector was plotted in Fig. 6. The propagation error rate in Fig. 6 is essentially the error rate generated by the standard method, since there is essentially no error rate associated with the proposed method.

Table 2

Case #	Theta, deg.	ω_0, rad/sec	ω_1, rad/sec^2	ω_2, rad/sec	ω_3, rad/sec	I_T, kg-m^2	I_S, kg-m^2
1	30	60	0	0	25	10	15
2	30	60	0	0	25	10	5
3	60	45	2	1	25	20	10
4	75	75	2	2	80	10	30
5	50	25	4	0.5	60	30	10

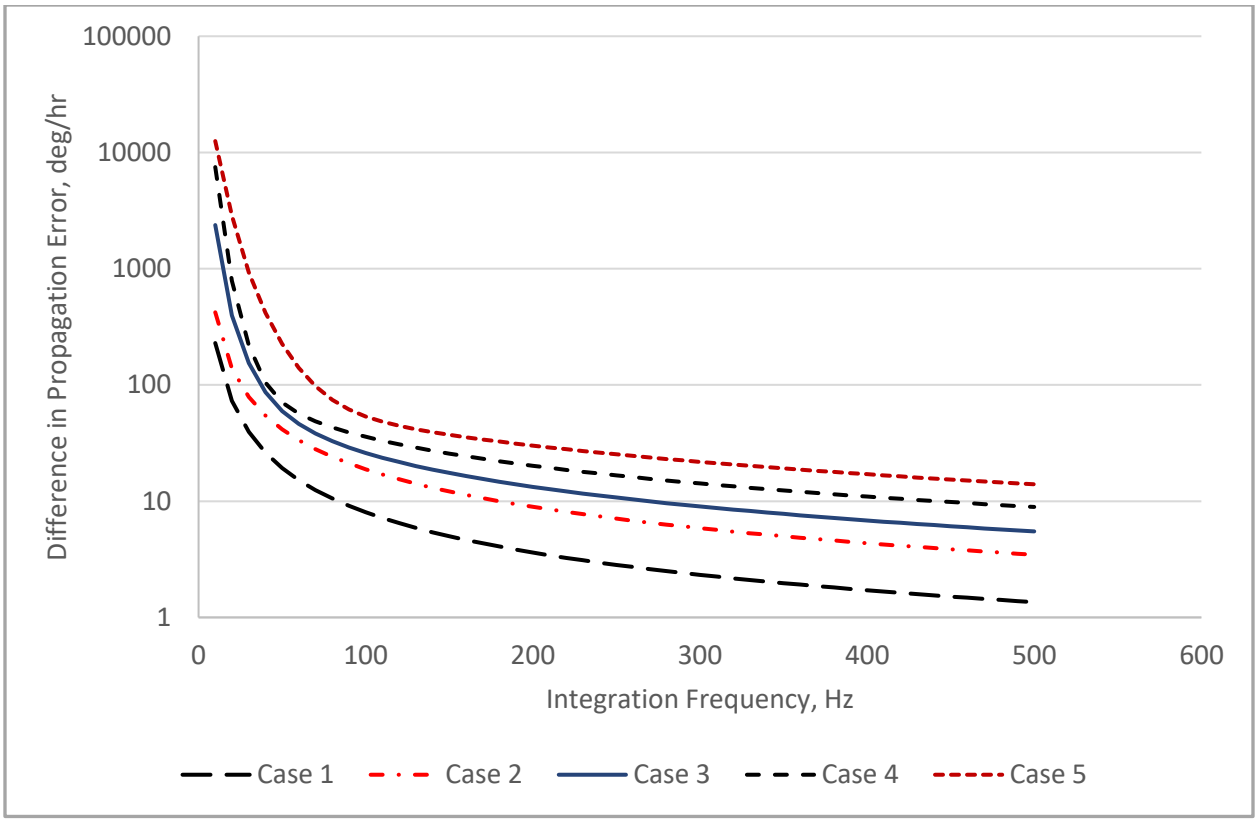

Fig. 6 Difference in propagation error between the new method and a standard method for an axisymmetric vehicle having parameters given in Table 2.

8. Conclusion

A new analytical method to compute the slewing transformation of an axis that moves along a conical trajectory centered on a fixed axis was developed. The result was used to formulate the propagation algorithm for a slewing angular rate vector using the slewing and rotational transformations of a single axis. It was shown that when the slew rate of the angular rate vector has a fixed orientation in the body frame and has a magnitude proportional to the angular rate vector magnitude, the attitude can be propagated with only numerical roundoff error, even for time dependent angular rate. In this case, the axis slews in synchronous motion with the angular rate vector, which permits both the slewing transformation and the rotational transformation to be evaluated with no error. Since the total transformation is the product of the slewing and rotational transformations, the resulting total transformation has no error. This new attitude propagation algorithm was applied to the case of pure coning motion and the propagation of an axisymmetric vehicle. The angular momentum vector is aligned with the inertial axis used in the propagation algorithm of the axisymmetric vehicle. The total transformation has two equivalent solutions, since it was shown in an earlier work that the slewing and rotation transformations commute when the slewing trajectory is fixed and the axis of the rotational transformation is accounted for. Thus, the slewing transformation can occur before or after the rotational transformation. The solution with the rotational transformation occurring before the slewing transformation is in agreement with earlier works, which serves to validate both this new method and the earlier methods. The other solution is a new finding of this work.

The algorithms were used in numerical simulations to demonstrate their validity. Results for several cases involving time dependent slew rate of a single axis were obtained using the current proposed method and compared to a standard propagation method. In addition, the attitude of an axisymmetric vehicle when driven by

a time dependent angular rate vector was computed using the proposed method and compared to results from a standard propagation method. For each numerical test, the higher the integration frequency of the standard propagation method, the closer its results were to that of the proposed method. Therefore, in all cases, the difference in propagation error was attributed to the standard propagation method, while the proposed propagation method was shown to be error free.

In summary, this work improves the accuracy of attitude propagation by determining that attitude propagation error arises in the slewing component of the attitude transformation. The error in the slewing transformation is eliminated by using the slew rate of the angular rate vector rather than the angular rate vector itself to compute the slewing transformation. Once the slewing error is removed, the rotational transformation and the total transformation are also error free. The analytical slewing transformation method developed and used in this work was also used to determine the precession of the Foucault Pendulum in a related work. It is likely that further discoveries and practical applications will result from the findings of this work.

References

Andrle, M. S., and Crassidas, J. L., 2013. Geometric Integration of Quaternions, Journal of Guidance Control and Dynamics, Vol. 36, No. 6.

Bortz, John, 1971. A new mathematical formulation for strapdown inertial navigation, IEEE Trans. Aerosp. Electro. Syst. AES-7 (1), 61-66.

Ishlinskii, A. Yu., 1952. The Mechanics of Special Gyroscopic Systems, Izd. Akad. Nauk, UkrSSR, Kiev.

Patera, R. P., 2010. Attitude propagation for a slewing angular rate vector, Journal of Guidance, Control and Dynamics, 33 (6), 1847-1855.

Patera, R. P., 2011. Attitude propagation for a slewing angular rate vector with time varying slew rate. In: Paper AAS 11-564 in Proceedings of AAS/AIAA Astrodynamics Specialist Conference (Astrodynamics 2011), pp. 2529-2546, Girdwood, Alaska, USA August 2011.

Patera, R. P., 2020a. Attitude kinematics using the slewing transformation of a single axis, Advances in Space Research, 66, 1460-1474.

Patera, R. P. 2020b. Kinematics of the Foucault Pendulum, viXra:2101.0150.

Patera, R. P. 2017. New fundamental parameters for attitude representation, Advances in Space Research, 60, 557-570.

Sveier, A., Sjoberg, A. M., Egeland, O., 2019. Applied Runge-Kutta-Munthe-Kaas Integration for the Quaternion Kinematics, Journal of Guidance, Control, and Dynamics, Vol. 42, No. 12.